Structural control of co-receptor binding in porphyrin–bipyridinium supramolecular assemblies

Maxwell J. Gunter,*[a] Tyrone P. Jeynes,[a] Martin R. Johnston,[a] Peter Turner[b] and Zhangping Chen[a]

[a] *Department of Chemistry, The University of New England, Armidale, NSW 2351, Australia*
[b] *School of Chemistry, The University of Sydney, NSW 2006, Australia*

A new series of porphyrin-based receptors for the bipyridinium ions paraquat and diquat, consisting in each case of a porphyrin with an over-arching dibenzo-crown ether, and related structures with hydroquinol-containing polyether straps is described. In all cases, the appended superstructure is connected to the porphyrin *via* ether linkages from the *o*-positions of the *meso*-aryls of the octaalkyl-5,15-diaryl substituted porphyrins. Solution studies of the complexes are compared to those of a previously reported set of related structures with amide linkages in place of the ethers and, at variance with the amide series, reveal conformations in which the complexed bipyridinium is parallel to the porphyrin sub-unit rather than perpendicular. Binding constants for all of the free-base and zinc porphyrin derivatives with both paraquat and diquat in various solvents allow the following principles to be established: (i) the binding strength decreases with increasing solvent polarity, (ii) there is little difference in the binding strength between the free base and zinc derivatives for a given receptor, (iii) binding is stronger for the more constrained 4(i) compared to the looser 4(ii), (iv) in general, paraquat binds more strongly than diquat, (v) the single-strapped analogues 6 are relatively ineffective as receptors for these bipyridinium guests, (vi) for a given sized dibenzo-crown ether cap or polyether strap, the substitution of ether linkages for the amide linkages in the related family of receptors 1 results in stronger binding. A similar binding motif is described for a naphthoquinol-strapped porphyrin 5. The solution studies are supported by X-ray crystal structures of two of the paraquat complexes which indicate that the guest is held by face-to-face π–π interactions with the porphyrin, by C–H · · · O hydrogen bonds, by electrostatic forces, and by either face-to-face π-stacking with the hydroquinol unit or by edge-to-face interactions in the case of the dibenzo-crown strapped molecule.

In the search for efficient ways to exploit the energy of visible light, supramolecular assemblies with addressable photo-active components have often been the system of choice.[1–6] Within these, porphyrins continue to feature prominently as components of photodynamic systems that seek to mimic both rapid electron-transfer processes and efficient charge separation, both of which are essential features of photosynthetic model systems and artificial photosynthesis devices.[7–10] Studies with covalently-linked donor–acceptor model systems abound,[6,11,12] and these have enabled a rationalisation of the structural effects and other parameters necessary to achieve useable efficiencies in charge-separating electron transfer events. Others have concentrated on the use of non-covalently linked donor–acceptor complexes, not necessarily porphyrinic,[13–19] to overcome many of the restrictions associated with covalently linked systems, not the least of which is the considerable synthetic challenge and the inherent inflexibility in design modification of the assembled molecules. One particular approach adopted by us[20–23] and others[19,24–33] has been to utilise supramolecular assemblies with photoactive porphyrins and electron acceptors as components.

We have shown[20–23] that systems comprising a porphyrin with an appended dibenzo-crown ether of appropriate dimensions, exemplified by **1**, can act as efficient receptors for bipyridinium guests, including paraquat, diquat and a related platinum complex. Nevertheless, we were also able to demonstrate that the binding ability was limited by the extent of conformational restriction imposed by the amide functionality linking the crown ether unit with the porphyrin.[23] Other factors were also investigated, and the following design principles emerged: (i) two polyether straps lead to stronger binding than a single strapped analogue such as **2**, (ii) in the absence of any polyether strap, such as in **3**, binding was minimal, (iii) reduction of the amide bond resulted in stronger binding of the bipyridinium guests. These variations have produced an interesting case for a study of the fine balance and interplay between *preorganisation* and *reorganisation* in designing specific receptors for a family of guest molecules.

Nevertheless, it became apparent that the amide bond was too complicating a factor in any rational design strategy which might seek a relationship between the binding strength and the efficiency of charge escape during photoinduced electron transfer processes in a photophysical investigation of the series of structures. We thus embarked on a program of synthesis for the related molecular receptors **4** in which all linkages within the superstructure above the base porphyrin are ethers.

At the same time, we have also included in this study the receptors **5** which have been utilised previously by us for the construction of porphyrin catenanes.[34] These represent quite a different series in that the porphyrin subunit is strapped by a hydroquinol- or naphthoquinol-containing polyether; in these cases the binding motif is restrained to a co-parallel orientation of porphyrin, quinol and bipyridinium guest. So while structures **1** and **4** were expected to enfold a bipyridinium guest in a manner analogous to that of the non-porphyrinic parent molecules (such as bis-*m*-phenylene-3*n*-crown-*n* derivatives, where the crown host over-arches the guest in a 'head-phone' fashion[35–39]), structures **5** resembled the *p*-phenylene or hydroquinol analogues bis-*p*-phenylene-3*n* + 4-crown-*n*, where the guest is threaded through the annulus of the crown ether.[39–43] The overall design strategy was then to enforce a perpendicular orientation of the bipyridinium guest with respect to the por-

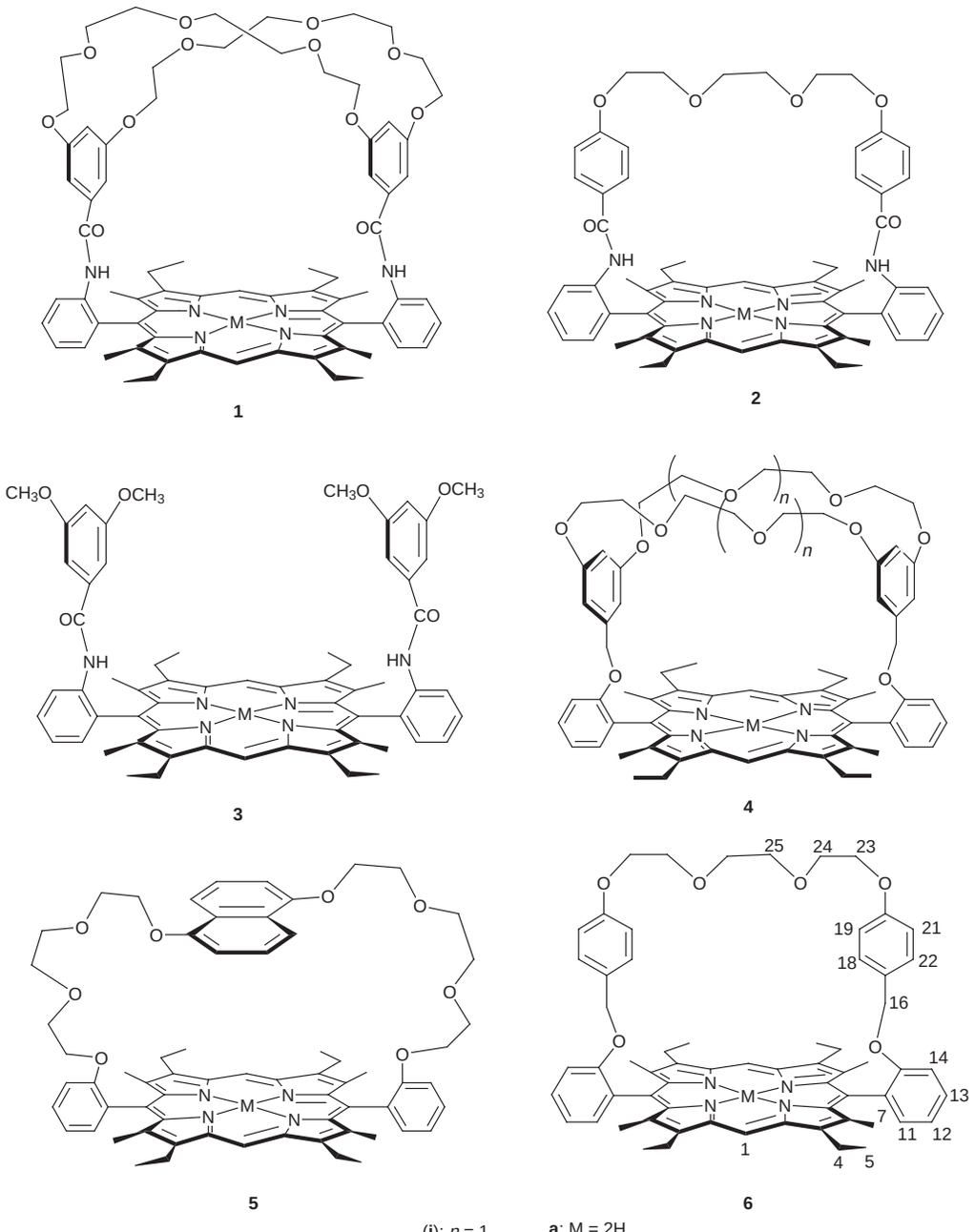

phyrin for **1**, and thus by analogy for **4**, while a parallel orientation is dictated by **5** as shown in Fig. 1 (structures **1**·BP^{2+}, **4**·BP^{2+} and **5**·BP^{2+}). Nevertheless, both series of receptors serve a similar function, which is to create a binding site for an acceptor bipyridinium contiguous to a photoactive porphyrin. Both series of molecules then were to have allowed a comparison of receptor design and binding strength in relation to the photophysical studies that we are currently undertaking, and which are reported elsewhere.[25,44]

However, as will be seen, the solid state and solution studies of the complexes of **4** confound our predictions of the binding geometry of the encapsulated guest, and indeed are at variance with the structures predicted by solution studies of **1**. It appears that an apparently subtle change from amide to ether linkages in the porphyrin superstructure results in a surprising orientation change of the included guest molecules from perpendicular to parallel, as illustrated in Fig. 1 for **4**·BP^{2+}.

In this paper, we report the synthetic strategies for the series of receptors **4**, and the results of a detailed investigation of the binding of paraquat and diquat guests, both in solution and in the solid phase. These results complement the recently reported photodynamic studies on several of the molecules reported here,[44] and are a prelude to further in-depth studies of their photophysical and electrochemical behaviour.

Results and discussion

Synthesis and solution conformations

An additional advantage of these ether-connected superstructured porphyrins and the previously reported amide-linked analogues was the relative ease of synthesis. Rather than rely on a tedious procedure to isolate the α,α-atropisomer of the *o*-diaminoporphyrin precursor,[45] the crown-ether straps were incorporated such that the porphyrin was synthesised underneath the pre-assembled straps as indicated in Scheme 1. Furthermore, a direct synthesis of the crown ether **7** from methyl 3,5-dihydroxybenzoate, rather than a stepwise procedure *via* the monoprotected derivative as reported by us earlier,[23] allowed easy access to multi-gram quantities of material. Reduction of the ester function, and reaction with salicylaldehyde produced the dialdehyde **10**, which was then condensed with the dipyrrylmethane **11**, to give the required

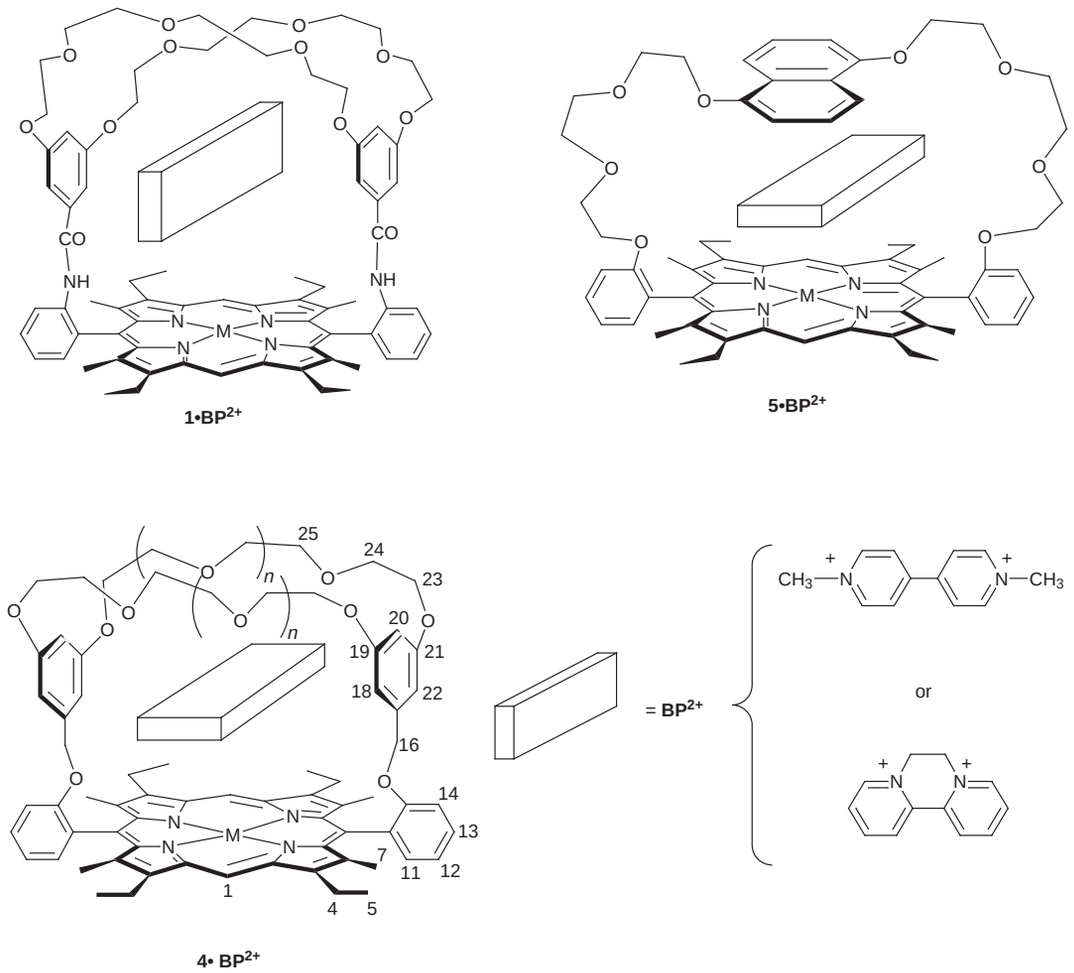

Fig. 1 Cartoon representing the possible binding geometries for bipyridinium dications paraquat and diquat in these porphyrin receptors. The non-systematic numbering shown is that used in the description of the NMR spectra

porphyrin **4** in good yield. The single-strapped derivative **6** was easily synthesised as outlined in Scheme 2, while the naphthoquinol-strapped **5** was synthesised as reported earlier.[34]

The solution structures of the receptors could be established from NMR spectroscopy, which in each case implied a conformation in which the crown ether chains were folded inwards over the face of the porphyrin. This is consistent with the observed chemical shifts, where significant shielding is experienced by all of the ethylene groups of the polyether chains.

Complexation studies

On the addition of the bipyridinium species paraquat (1,1′-dimethyl-4.4′-bipyridinium) or diquat (6,7-dihydrodipyrido-[1,2-*a*:2′,1′-*c*]pyrazinediium), solubilised as their hexafluorophosphate salts, to solutions of the receptors **4** or **6** in hexadeuteroacetone, it was immediately apparent from the ^{1}H NMR spectra that strong binding had occurred. Equimolar solutions of host and guest revealed significant shifts in the NMR spectra of both species. The directions of the ^{1}H NMR resonance shifts and their magnitudes allowed both their geometry to be established and the strength of binding (the association constant K) to be estimated. The direction and magnitudes of the ^{1}H shifts are collected in Table 1.

Unlike the previously reported porphyrin–crown ether receptors with in-built amide linkages, where the bipyridinium units were oriented perpendicular to the porphyrin, in these cases it is clear that the paraquat complexes have the parallel geometry shown in Fig. 1. This is also consistent with the solid-state structure shown below (Fig. 2), showing the bipyridinium unit parallel to the porphyrin, and presumably stabilised, *inter alia*, by face-to-face π–π interactions with the porphyrin, and edge-to-face interactions with the lateral benzo-groups of the crown. The overall pattern of shifts for protons of both the guest and host molecules closely parallel those of the related hydroquinol and naphthoquinol strapped porphyrins that we have previously reported, and are at variance with the alternative amide-linked dibenzo-crown analogues. In the former, a face-to-face orientation of host and guest is mandatory, whereas for the latter, we have argued a perpendicular binding motif for the bipyridinium guests on the basis of the ^{1}H NMR shifts.[23]

For example, the *meso* protons H1 and the inner pyrrolic NH protons (in the free base derivatives **4a**) are shielded by the complexed paraquat or diquat. Nevertheless, the crown ether methylene protons are all significantly deshielded on binding by either of the two bipyridiniums. As before, we rationalise this in terms of a shift in the geometry of the uncomplexed crowned porphyrin as the guest is bound: initially, the lateral benzo-rings and the crown resonances are strongly shielded by the porphyrin as a result of an enfolded conformation to maximise π–π interactions of the aromatic rings and the porphyrin. On complexation, the crowns are forced outward and upward to accommodate the parallel guest (a movement not unlike a flower opening from a bud to a bloom); the strong shielding by the porphyrin is now replaced by the weaker shielding of the paraquat or diquat, and the net result is an overall deshielding of the methylene protons.

For the single-strapped derivatives **6**, the binding is weaker and thus the shifts are smaller for the complexes measured at 1:1 molar ratios. Nevertheless, the same trends are followed, indicating a similar binding geometry.

We have previously reported on the binding characteristics of

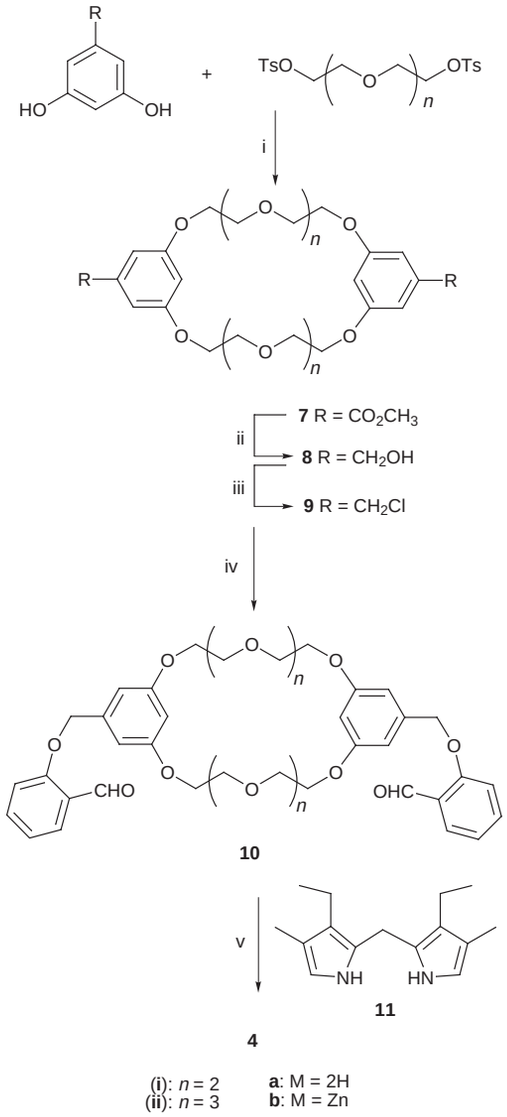

Scheme 1 *Reagents and conditions*: i, NaH–THF; ii, $LiAlH_4$, THF; iii, $SOCl_2$, pyridine, C_6H_6; iv, salicylaldehyde, K_2CO_3, MeCN; v, CCl_3CO_2H, MeCN–THF, then *o*-chloranil, then $ZnOAc/MeOH/CH_2Cl_2$ for **b**

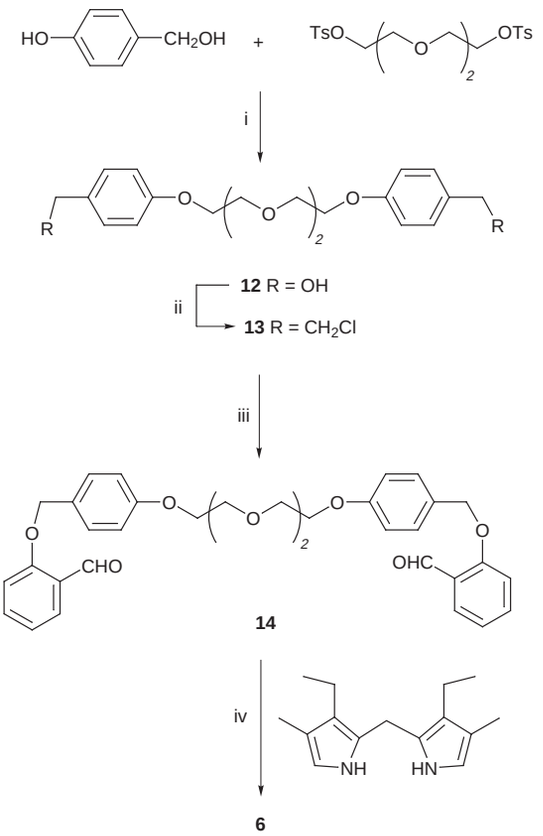

Scheme 2 *Reagents and conditions*: i, K_2CO_3, MeCN; ii, $SOCl_2$, pyridine–C_6H_6; iii, salicylaldehyde, MeCN, K_2CO_3; iv, CCl_3CO_2H, MeCN–THF, then *o*-chloranil, then $ZnOAc/MeOH/CH_2Cl_2$ for **b**

the naphthoquinol-strapped porphyrin **5**[34] and several related hydroquinol derivatives. In these cases, the orientation of the guest is firmly established and the complex has the geometry shown in Fig. 1. This is confirmed by the crystal structure discussed below. For comparison, the association constant for **5** was also measured in solvents of different polarity and, as for **4** and **6**, it can be seen that an increase in solvent polarity leads to a decrease in association constant. This is consistent with an entropic barrier associated with a highly solvated polar host and guest compared to the complex.[46–48] The values for **4(i)b** and **5** also compare favourably with those calculated from fluorescence measurements in acetonitrile, 8×10^4 and 1×10^4 M^{-1}, respectively.[44]

Table 2 contains the association constants for the various complexes. Several trends are evident: (i) as we have demonstrated previously for a related set of receptors, the binding strength decreases with increasing solvent polarity, (ii) there is little difference in the binding strength between the free base and zinc derivatives for a given receptor, (iii) binding is stronger for the more constrained **4(i)** compared to the looser **4(ii)**, (iv) in general paraquat binds more strongly than diquat, (v) the single-strapped analogues **6** are relatively ineffective as receptors for these bipyridinium guests, (vi) for a given sized dibenzo-crown ether cap or polyether strap, the substitution of ether linkages for the amide linkages in the related family of receptors **1** results in significantly stronger binding, (vii) the naphthoquinol-strapped derivatives **5** are equally effective as receptors for bipyridinium dications, and the same geometry is maintained in these and related complexes.

Solid state structures

In a complementary and confirmatory study, single crystals of the paraquat complexes **4(i)b·PQ**$^{2+}$ and **5b·PQ**$^{2+}$ were subjected to X-ray crystallography.

Complex 4(i)b·PQ^{2+}. Selected geometrical details for complex **4(i)b·PQ**$^{2+}$ are listed in Table 3 and labelled ORTEP[49] depictions are provided in Figs 2 and 3. It is apparent that the dicationic paraquat substrate is principally retained within the cavity of the porphyrin by π-stacking of the pyridinium residues and the porphyrin core, by C–H···O interactions between the paraquat and the crown oxygens, and by edge-to-face π-interactions between the guest and the flanking aryl units of the appended dibenzo-crown. The substrate is centrally nestled across the porphyrin core with the angle between the N(6)–N(7) paraquat axis and the N(1)–N(3) porphyrin axis being 14.5(1)°. The distances between the N(3) pyrrole least-squares plane and the paraquat N(7), C(79), C(80), C(81), C(82) and C(83) sites are 3.589(2), 3.840(2), 3.740(2), 3.789(1), 3.149(1) and 3.250(1) Å respectively. The paraquat principal axis is inclined at 3.36(1)° with respect to the porphyrin least squares plane. However, neither the paraquat nor the porphyrin are exactly planar, and it appears that face-to-face interactions are maximised as far as possible between host and guest. For example, the dihedral angle between the least-squares plane of the N(3) pyrrole and the N(7) pyridinium residue is 15.18(4)°, while the dihedral angle formed between the least-squares planes of the N(1) pyrrole and the N(6) pyridinium paraquat residue is 7.61(4)°. The distances between this pyrrole least-squares plane and the paraquat N(6), C(73), C(74), C(75),

Table 1 Selected ^{1}H NMR resonance shifts on binding of the paraquat and diquat dication guest by the hosts in equimolar solutions of host and guest[a]

Host Guest	**4(i)a** PQ^{2+}	**4(i)b** PQ^{2+} [b]	**4(ii)a** PQ^{2+}	**4(ii)b** PQ^{2+}	**6a** PQ^{2+}	**6b** PQ^{2+} [e]	**4(i)a** DQ^{2+}	**4(i)b** DQ^{2+} [c]	**4(ii)a** DQ^{2+}	**4(ii)b** DQ^{2+}	**6a** DQ^{2+} [d]	**6b** DQ^{2+} [e]
H-1	9.93	9.79	10.11	9.93	10.26	10.04	9.93	9.89	10.21	10.03	10.26	10.06
	(−0.26)	(−0.26)	(−0.14)	(−0.24)	(+0.02)	(−0.03)	(−0.26)	(−0.26)	(−0.04)	(−0.14)	(+0.02)	(−0.01)
H-11	7.80	7.66	7.64	7.45	7.63	7.51	7.71	7.55	7.71	7.54	7.60	7.49
	(−0.08)	(−0.16)	(−0.25)	(−0.39)	(+0.01)	(−0.01)	(−0.17)	(−0.17)	(−0.18)	(−0.30)	(−0.02)	(−0.02)
H-14	7.81	7.79	7.78	7.75	7.72	7.73	7.80	7.80	7.71	7.67	7.71	7.73
	(+0.22)	(+0.22)	(+0.18)	(+0.22)	(+0.06)	(+0.06)	(+0.21)	(+0.21)	(+0.11)	(+0.14)	(+0.05)	(+0.06)
H-16	5.26	5.30	5.26	5.28	5.28	5.31	5.29	5.35	5.20	5.18	5.26	5.28
	(+0.31)	(+0.31)	(+0.19)	(+0.32)	(+0.06)	(+0.08)	(+0.34)	(+0.34)	(+0.13)	(+0.22)	(+0.04)	(+0.05)
H-18, -22	6.34	6.37	6.02	6.09	6.56	6.73	6.32	6.41	5.76	6.03	6.50	6.67
	(+0.82)	(+0.82)	(+0.68)	(+0.41)	(+0.03)	(+0.10)	(+0.80)	(+0.80)	(+0.42)	(+0.35)	(−0.03)	(+0.03)
H-19, -21	—	—	—	—	5.87	6.06	—	—	—	—	5.94	6.09
					(−0.19)	(−0.06)					(−0.12)	(−0.03)
H-20	5.13	5.12	5.19	5.18	—	—	5.33	5.35	5.50	5.56	—	—
	(−0.39)	(−0.39)	(−0.36)	(−0.56)			(−0.19)	(−0.19)	(−0.05)	(−0.18)		
H-23	3.24	3.2[g]	3.05	3.10	3.42	3.50	3.37	3.45	2.80	3.24	3.63	3.60
	(+0.49)	(+0.16)	(+0.87)	(−0.02)	(−0.09)	(−0.06)	(+0.62)	(+0.43)	(+0.62)	(+0.12)	(+0.12)	(+0.05)
H-24	3.41	3.43	3.20	3.25	3.37	3.36	3.37	3.56[h]	2.80	3.07	3.43	3.40
	(+0.74)	(+0.44)	(+1.28)	(+0.64)	(−0.01)	(−0.01)	(+0.70)	(+0.62)	(+0.88)	(+0.48)	(+0.05)	(+0.03)
H-25	3.51	3.53	3.46	3.38	3.33	3.27	3.51	3.45[h]	3.07	2.6[g]	3.38	3.31
	(+0.57)	(+0.54)	(+0.94)	(+1.86)	(+0.05)	(+0.01)	(+0.58)	(+0.50)	(+0.55)	(+1.09)	(+0.10)	(+0.05)
H-26	—	—	3.52	3.38	—	—	—	—	3.23	2.6[g]	—	—
			(+0.67)	(+2.16)					(+0.40)	(+1.38)		
Pyrrole NH	−3.47	—	−2.70	—	−2.45	—	−3.56	—	−2.58	—	−2.3[g]	—
	(−1.00)		(−0.38)		(−0.17)		(−1.09)		(−0.26)		(−0.03)	
2′,6′ (PQ^{2+})/	7.29	7.25	7.09	7.09	7.72	8.48	4[g]	—[f]	5.02	—[f]	6.44[g]	7.35[g]
3′,3″ (DQ^{2+})	(−2.08)	(−2.12)	(−2.28)	(−2.28)	(−1.65)	(−0.95)	(−5.26)		(−4.24)		(−2.82)	(−1.93)
3′,5′ (PQ^{2+})/	3.78	—[f]	4.25	4[g]	6.56	7.49	7.16	7.14	7.13	7.4[g]	7.60[g]	8.09
4′,4″ (DQ^{2+})	(−5.04)		(−4.57)	(−4.8)	(−2.26)	(−1.40)	(−1.95)	(−1.95)	(−1.98)	(−1.67)	(−1.51)	(−0.98)
5′,5″ (DQ^{2+})	—	—	—	—	—	—	7.5[g]	7.4[g]	7.67	7.6[g]	7.92	7.97
							(−1.11)	(−1.11)	(−0.94)	(−0.96)	(−0.69)	(−0.59)
6′,6″ (DQ^{2+})	—	—	—	—	—	—	6.79	6.7[g]	8.38	7.98	8.86	8.96
							(−2.73)	(−2.73)	(−1.14)	(−1.53)	(−0.66)	(−0.55)
$^+$NMe(PQ^{2+})/	4.12	4.18	3.95	3.94	3.88	4.14	2.65	2.5[g]	4.21	3.58	5.06	4.90
$^+$NCH$_2$(DQ^{2+})	(−0.62)	(−0.56)	(−0.79)	(−0.80)	(−0.86)	(−0.40)	(−3.05)	(−3.05)	(−1.49)	(−1.97)	(−0.64)	(−0.65)

[a] Spectra recorded at 300 K in [^{2}H$_6$]acetone–$CDCl_3$ (14%) using residual acetone as reference (δ 2.05). Porphyrin concentration approximately 3 mM; chemical shifts (ppm) of equimolar solutions of the porphyrin host and the guest, recorded under conditions of fast exchange, *i.e.* with averaged signals of host and guest in bound/unbound equilibria. Values in parentheses ($\Delta\delta$) indicate differences in chemical shift between the complexed and uncomplexed host and guest measured at 1:1 molar ratio, with a positive sign indicating deshielding and a negative sign indicating shielding. [b] Porphyrin concentration approximately 1 mM. [c] Porphyrin concentration approximately 2 mM. [d] Porphyrin concentration approximately 4 mM. [e] Spectra were recorded in [^{2}H$_6$]acetone–[^{2}H$_6$]DMSO (20%), porphyrin concentration approximately 3 mM. [f] Resonance not observed. [g] An exact chemical shift could not be measured since this broad peak was obscured by other resonances. [h] Assignment ambiguous—these entries may be interchanged.

Table 2 Binding constants (K_a) for several crown ether strapped porphyrin hosts with paraquat and diquat guests determined by ^{1}H NMR titration in CD_3COCD_3–$CDCl_3$ (14%)

	K_a (M^{-1})	
Host	$PQ(PF_6)_2$	$DQ(PF_6)_2$
1[a]	5.0×10	—[a]
4(i)a	2.4×10^5	2.0×10^4
4(i)b	8.1×10^5[e]	1.2×10^5
4(ii)a	6.2×10^4	2.2×10^3
4(ii)b	5.5×10^4	1.4×10^3
4(i)a[b]	1.2×10^2	—
4(ii)a[b]	1.9×10	—
6a	5.6×10^2	6.3×10^2
6b[c]	4.9×10^2	2.5×10^2
5b[d]	2.1×10^4	—
5b[c]	2.3×10^3[f]	—

[a] Measured in CD_3COCD_3; no significant binding of DQ^{2+} detected, see ref. 23. [b] ^{1}H NMR titration carried out in CD_3SOCD_3–$CDCl_3$ (14%). [c] ^{1}H NMR titration carried out in CD_3COCD_3–CD_3SOCD_3 (20%) for solubility reasons. [d] Measured in [^{2}H$_7$]dimethylformamide, ref. 34. [e] Value measured in CH_3CN by fluorescence techniques 8.0×10^4, ref. 44. [f] Value measured in CH_3CN by fluorescence techniques 1.0×10^4, ref. 44.

Table 3 Selected geometrical details for complex **4(i)b**·PQ^{2+} and complex **5b**·PQ^{2+}

4(i)b·PQ^{2+}	**5b**·PQ^{2+}
Bond lengths (Å)	
Zn(1)–N(1) 2.068(3)	Zn(1)–N(1) 2.06(4)
Zn(1)–N(2) 2.061(3)	Zn(1)–N(2) 2.06(4)
Zn(1)–N(3) 2.060(3)	Zn(1)–N(3) 2.10(3)
Zn(1)–N(4) 2.068(3)	Zn(1)–N(4) 1.98(4)
Zn(1)–N(5) 2.211(4)	Zn(1)–O(7) 2.20(3)
Bond angles (°)	
N(1)–Zn(1)–N(2) 91.4(1)	N(1)–Zn(1)–N(2) 94(1)
N(1)–Zn(1)–N(3) 165.6(1)	N(1)–Zn(1)–N(3) 167(1)
N(1)–Zn(1)–N(4) 86.4(1)	N(1)–Zn(1)–N(4) 82(1)
N(2)–Zn(1)–N(3) 86.1(1)	N(2)–Zn(1)–N(3) 84(1)
N(2)–Zn(1)–N(4) 159.5(1)	N(2)–Zn(1)–N(4) 165(1)
N(3)–Zn(1)–N(4) 90.9(1)	N(3)–Zn(1)–N(4) 95(1)
N(1)–Zn(1)–N(5) 94.2(1)	O(7)–Zn(1)–N(1) 98(1)
N(2)–Zn(1)–N(5) 102.2(1)	O(7)–Zn(1)–N(2) 100(1)
N(3)–Zn(1)–N(5) 100.2(1)	O(7)–Zn(1)–N(3) 93(1)
N(4)–Zn(1)–N(5) 98.3(1)	O(7)–Zn(1)–N(4) 93(1)

C(76) and C(77) sites are 3.120(1), 3.314(2), 3.244(2), 3.096(2), 2.958(2) and 3.002(1) Å respectively. The N(1) pyrrole to N(6) pyridinium distances are significantly less than the carbon-carbon van der Waals contact distance of around 3.5 Å. The closer contact between the N(6) pyridinium and the porphyrin core compared to that of the N(7) pyridinium would appear to be a consequence of the O(4) to O(6) crown ether segment being folded down towards the porphyrin plane. Consequently

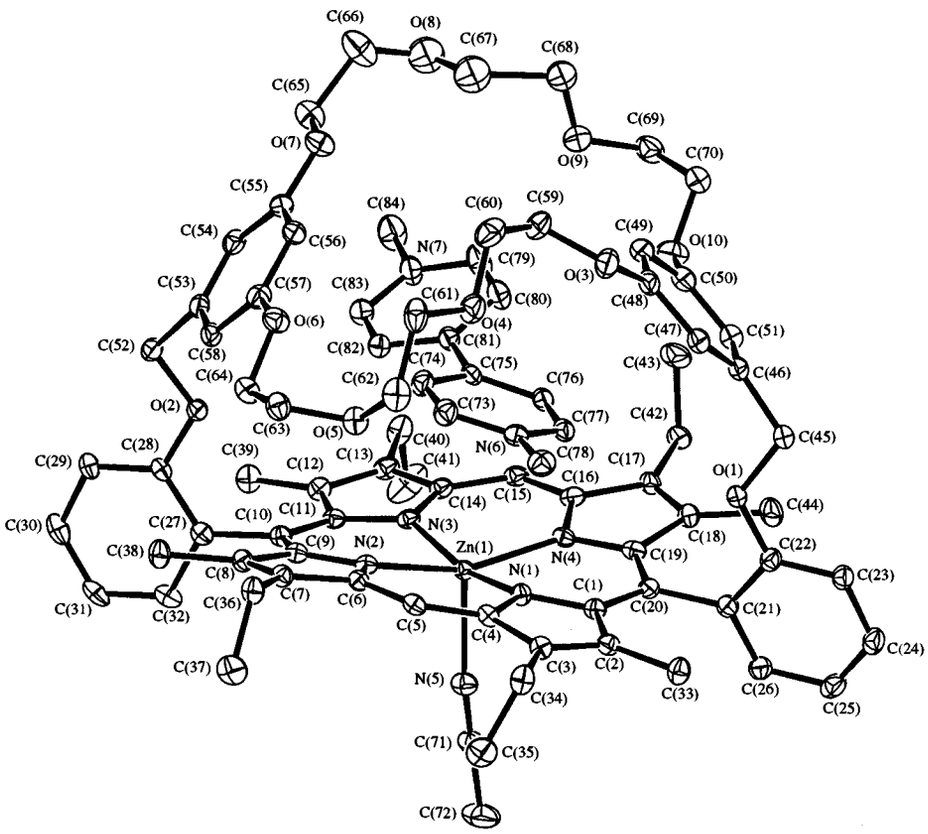

Fig. 2 A labelled ORTEP projection of complex **4(i)b·PQ**$^{2+}$, with thermal ellipsoids at the 25% level

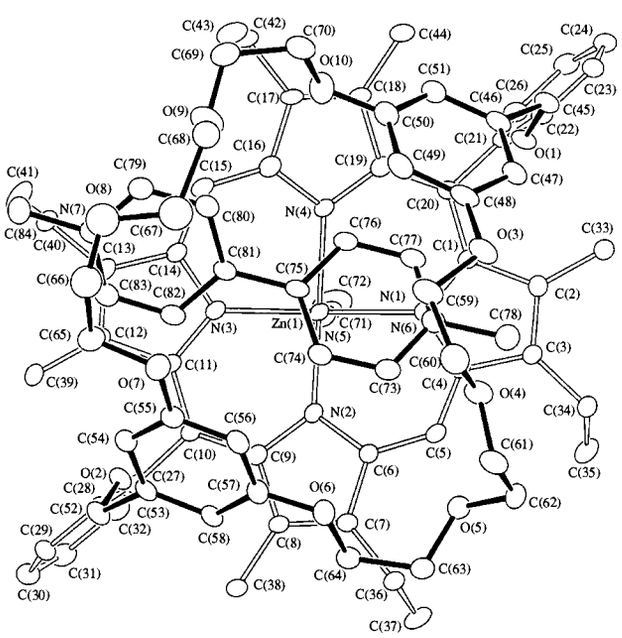

Fig. 3 A labelled ORTEP depiction of complex **4(i)b·PQ**$^{2+}$, viewed approximately down the normal to the porphyrin core plane and showing the placement of the substrate with respect to the porphyrin

the O(4)–C(73), O(4)–C(78), O(5)–C(73) and C(47)–C(77) distances are 3.339(6), 3.330(6), 3.197(6) and 3.355(7) Å respectively. In contrast there are only two notably close contacts between the substrate and the crown ether on the N(3) side of the complex. There is a 3.186(6) Å separation between O(9) and C(80) and a 3.191(7) Å distance between O(9) and C(79). The folding of the crown ether O(4) to O(6) segment towards the porphyrin core is imposed by the close proximity of the porphyrin of a neighbouring symmetry related complex. The distance between C(61) of complex **4(i)b·PQ**$^{2+}$ and C(17) of the symmetry related complex is 3.583(7) Å.

The pyridinium residues of the paraquat substrate are rotated about the C(75)–C(81) axis such that the C(74)–C(75)–C(81)–C(82) torsion angle is −34.7(7)°, and this rotation approximately matches the porphyrin core C(1)–N(1)–N(3)–C(14) torsion angle of −14.8(5)°. In general, porphyrin cores adopt one of two conformational forms;[50] the *sad* conformer has pyrrole residues that are alternately tilted up and down with respect to the pyrrole nitrogen least squares plane and the *ruf* conformer has opposing pyrrole residues rotated about the nitrogen-nitrogen axis. The core of complex **4(i)b·PQ**$^{2+}$ appears to be an admixture of the *sad* and *ruf* conformations, with the N(2) and N(4) pyrrole residues having a more *sad* like disposition than the principally *ruf* disposition of the N(1) and N(3) pyrroles. The N(1) pyrrole is however slightly tilted and this is probably a response to close contact with the substrate that is imposed by the folding of the O(4) to O(6) segment of the crown ether.

Although there are several structures reported for free base and nickel 5,15-diaryloctaalkylporphyrins, there is only limited information on zinc derivatives. We have previously reported the structures of the free-base hydroquinol-strapped analogues of **5**,[23] and Smith and co-workers[51] have undertaken a structural investigation of a series of nickel and free-base derivatives of related, but not strapped, porphyrins. The conclusions from this study were that the two *meso* aryl substituents and eight β-substituents on a porphyrin do not impose any intrinsic distortion of the porphyrin core. As a closest analogy for the present structures described here, Anderson *et al.*[52] have reported a cyclic zinc porphyrin trimer, cyclotris[2,8,12,18-tetramethyl-3,7,13,17-tetraethylporphyrin-10,20-bis(*m*-phenylene)](buta-1,3-diyne-1,4-diyl)pyridylzinc, in which the porphyrin subunits are linked *via* the *meta* carbon of the phenyl residues of the porphyrin. Each of the zinc atoms is five coordinate, with the axial ligand being pyridine. Interestingly one of the porphyrins in the trimer has a pure *ruf* core conformation and the other

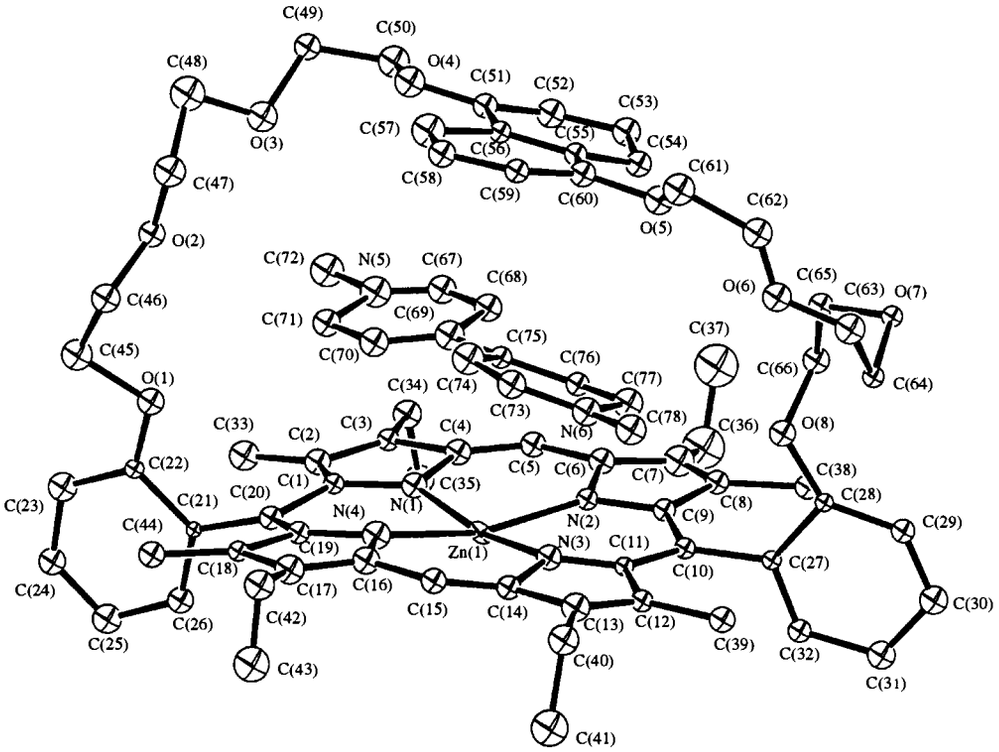

Fig. 4 A labelled ORTEP projection of complex **5b·PQ**$^{2+}$, with thermal ellipsoids at the 10% level

two have *sad* core conformations. In the porphyrin subunit of the trimer with the *ruf* core the pyrrole nitrogen deviations from the pyrrole nitrogen least-squares plane are ±0.005(1) Å and the zinc is displaced 0.325(1) Å from that plane. In the *sad* porphyrins the deviations are 0.052(1), −0.051(1), 0.049(1) and −0.050(1) for the nitrogens of one *sad* core and −0.067(1) 0.066(1), −0.066(1) and 0.068(1) Å for the nitrogens of the second *sad* core. The zinc distances from the respective nitrogen least-squares planes of the *sad* core porphyrins are 0.299(1) and 0.325(1) Å. In complex **4(i)b·PQ**$^{2+}$ the nitrogen deviations from the pyrrole nitrogen least-squares plane are −0.0537(1), 0.0540(1), −0.0543(1) and 0.0539(1) Å and the zinc is displaced 0.315(1) Å from this plane. The acetonitrile axial ligand in a complex is a significantly weaker ligand than pyridine and it is not surprising that in the complex **4(i)b·PQ**$^{2+}$ zinc displacement from the coordination least-squares plane of 0.315(1) Å is less than the 0.325(1) Å found in two of the three zinc porphyrins of the trimer. The smaller 0.299(1) Å zinc displacement in the trimer appears to be the result of inter-porphyrin π stacking interactions and is associated with a longer zinc to axial nitrogen distance than found in the other two trimer units. In the trimer, the zinc to axial nitrogen distances are 2.153, 2.154 and 2.175 Å, and in complex **4(i)b·PQ**$^{2+}$ the zinc to axial nitrogen distance is a little longer at 2.211(4) Å. The axial bond length difference again reflects different axial ligand field strengths. There are, to our knowledge, no reported structures of five coordinate zinc porphyrin complexes with acetonitrile as the axial ligand. There is however a six coordinate zinc porphyrin complex[53] with butyronitrile axial ligands, and not surprisingly the zinc to axial nitrogen distances in this complex are, at 2.51(4) and 2.59(3) Å, significantly longer than the axial bond in the five coordinate complex **4(i)b·PQ**$^{2+}$. In the five coordinate (acetonitrile)–bis{[(2-pyrrolyl)methylimino]-4,6-dimethylphenolato}-zinc(II) complex[54] the zinc–acetonitrile bond length is 2.114 Å. It may be worth noting that in complex **4(i)b·PQ**$^{2+}$ the angle formed between the axial nitrogen–zinc axis and the pyrrole nitrogen least-squares plane is 87.47(2)°.

There is evidence for aryl-aryl interactions between the lateral aryl groups of the dibenzo-crown and the included host in close contacts between C(46)–C(77) (3.405 Å), C(47)–C(77) (3.355 Å), C(48)–C(77) (3.401 Å) and C(50)–C(76) (3.380 Å). The least-squares plane of the N(6) pyridinium ring forms a dihedral angle of 32.11(3)° with the C(46)–C(51) least-squares plane of one of the lateral aryl groups, and the N(7) angle with this same aryl is 66.50(3)°. The C(53)–C(58) plane and the paraquat ring N(6) and N(7) dihedral angles are complementary at 66.36(3) and 32.26(3)°. An alternative view of this interaction are the short contact distances of 3.348 and 3.175 Å between C(76) and C(77) and the side aryl C(46)–C(51) plane, and the slightly longer but still significant distances of 3.484 and 3.315 Å between C(82) and C(83) and the opposite aryl group defined by the plane C(53)–C(58). Such a situation where the interacting aryl rings are angled to each other is common in many examples where aryl-aryl interactions have been invoked,[55] and several systematic studies have been carried out on the relationship between the geometric orientation and the attractive *vs*. repulsive interactions.[56–58] It is clear that the alignment of the two aryl groups in this case fall within the attractive region in a plot of electrostatic interaction as a function of orientation as described by Hunter and Sanders.[58]

Complex 5b·PQ^{2+}. The crystal structure for complex **5b·PQ**$^{2+}$ is of poor quality, but is nonetheless sufficiently well resolved to provide meaningful insights and informative comparisons with the structure of complex **4(i)b·PQ**$^{2+}$. Selected geometrical details are listed in Table 3 and numbered ORTEP[49] depictions of the complex are provided in Figs. 4 and 5. As Fig. 6 suggests, the complex **5b·PQ**$^{2+}$ crystal structure contains oligomeric chains of complexes in which the zinc of one complex is coordinated to O(7) on the strap of a second complex.

The tilting of the pyridinium components of the substrate with respect to each other in complex **5b·PQ**$^{2+}$ is similar to that in complex **4(i)b·PQ**$^{2+}$, with the C(70)–C(69)–C(75)–C(74) torsion angle being −26(9)°. The porphyrin core of complex **5b·PQ**$^{2+}$ is flatter than that of complex **4(i)b·PQ**$^{2+}$. The deviations of the nitrogens defining the pyrrole least-squares plane from that plane are −0.02(2), 0.02(2), −0.02(2) and 0.04(3) Å. The C(1)–N(1)–N(3)–C(14) torsion angle is 3(3)° and the C(6)–N(2)–N(4)–C(19) angle is 12(3)°. The dihedral angles formed between the pyrrole nitrogen least-squares plane and

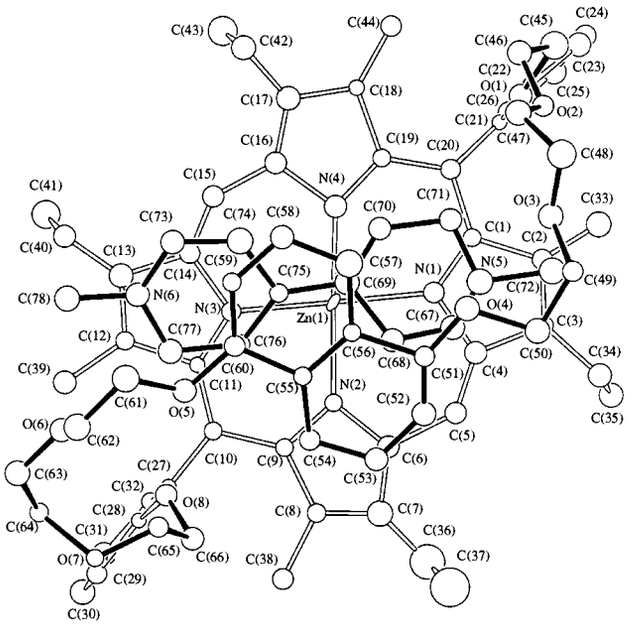

Fig. 5 A labelled ORTEP depiction of complex **5b·PQ^{2+}**, viewed approximately down the normal to the porhyrin core plane and showing the placement of the substrate with respect to the porphyrin

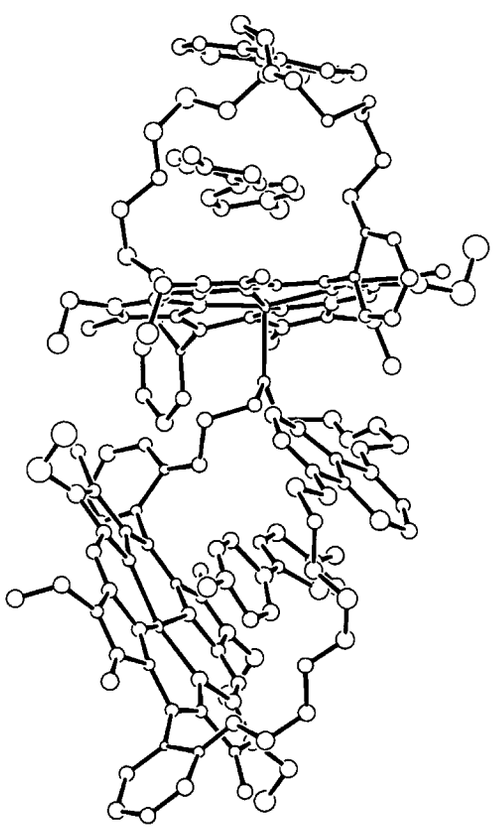

Fig. 6 An ORTEP depiction of complex **5b·PQ^{2+}**, showing two members of an oligomer formed by coordination of the O(7) of one complex to the zinc of a neighbouring complex

the individual N(1), N(2), N(3) and N(4) pyrrole least-squares planes are 4(1), 4(1), 4.9(8) and 4.4(9)° respectively. In complex **4(i)b·PQ^{2+}** the dihedral angles formed between the pyrrole nitrogen least-squares plane and the individual N(1), N(2), N(3) and N(4) pyrrole least-squares planes are 6.82(4), 9.66(4), 8.56(4) and 12.98(4)° respectively.

Interestingly, the angle formed between the N(5)–N(6) substrate axis and the N(1)–N(3) porphyrin axis of complex **5b·PQ^{2+}** is only 2.9°, in contrast to the 14.5° found in complex **4(i)b·PQ^{2+}**. The dihedral angle formed between the N(6) pyridinium residue's least-squares plane and the N(3) pyrrole least-squares plane is 16(1)°, whereas the dihedral angle between the N(5) pyridinium and N(1) pyrrole planes is 1(1)°. The dihedral angle formed between the N(6) pyridinium plane and the C(55) to C(60) naphthyl residues least-squares plane is 7(1)°. Thus the N(6) pyridinium is involved in π stacking interactions both with the N(3) pyrrole and with the naphthyl cap, as expected. As Fig. 5 indicates, the N(6) pyridinium is appropriately placed for an offset π stacking interaction with the C(55) to C(60) ring of the naphthyl cap. The C(75) site is 3.59(4) Å away from the C(55) to C(60) least-squares plane.

Conclusions

The solid state structures thus re-affirm the credibility of these polyether strapped porphyrins as effective receptors for bipyridinium dications. Furthermore they confirm the binding geometry and complexation strength deduced from the solution measurements. These factors taken together reinforce the paradigms that have now become firmly established within the concepts of supramolecular chemistry. That is, (i) effective binding of a substrate within a receptor is both entropically and enthalpically driven (binding strength decreases with solvent polarity), (ii) there needs to be a careful balance established between pre-organisation and reorganisation (these polyether-strapped derivatives are more effective than their more conformationally restricted amide-linked counterparts, but too long a strap leads to decreased binding strength), and (iii) an optimum complementarity between host and guest needs to be finely tuned with regards to the overall binding motif (for example the optimum number and orientation of C–H···O hydrogen bonds, and the orientation and π-electron density complementarity of π-donor and acceptors). This series nicely illustrates these concepts, and hence it is now possible to finely adjust these receptors to optimise the desired properties for a specific function. For example, we are using this series of molecules in a photophysical study to optimise charge escape and charge separation of donor and acceptor molecules on photoexcitation.[44]

Experimental

Synthetic procedures

All solvents were distilled before use: tetrahydrofuran and pyridine were distilled over $LiAlH_4$ under N_2. Benzene was distilled and dried over sodium wire; AR grade acetonitrile was dried over type 3 Å molecular sieves. Column chromatography on alumina was carried out using Aldrich aluminium oxide, activated, neutral (Brockmann I standard grade), and silica chromatography using Aldrich silica gel (grade 9385, 230–400 mesh). Chromatotron chromatography was carried out on a model 7924T Chromatotron using plates coated with 2 mm thick Merck silica gel 60 PF_{254} containing gypsum. Preparative TLC was performed on 20 × 20 cm plates coated with 0.5 mm thick Art. 7731 Kieselgel 60 G Merck silica. Analytical TLC was carried out on Merck Silica Gel 60 G_{254} pre-coated aluminium sheets.

NMR spectra were acquired using a 300 MHz Bruker AC 300 spectrometer at 300 K. Chemical shifts (δ) are reported in parts per million relative to residual solvent. ^{13}C Spectra were referenced against residual chloroform. COSY-45, one-bond C-H correlation, long-range C-H correlation (FLOCK), DEPT and NOESY two-dimensional NMR experiments employed the standard Bruker parameters. NOE difference and saturation transfer experiments utilised standard Bruker pulse programs. UV spectra were recorded on a Hewlett Packard 8452A diode array spectrometer.

Electrospray–MS were recorded at the Department of Medicinal Chemistry, Victorian College of Pharmacy, Monash

University. Microanalyses were performed at the Microanalytical Unit, Research School of Chemistry, Australian National University.

Melting points were determined using a Reichert melting point apparatus.

Dimethyl 1,4,7,10,17,20,23,26-octaoxa[10.10]metacyclophane-13,29-dicarboxylate 7(i)

A mixture of methyl 3,5-dihydroxybenzoate (12.5 g, 0.074 mol) and NaH (5.5 g, 0.229 mol) in dry tetrahydrofuran (250 ml) was heated at 60 °C for 25 min with stirring under N_2. Then a solution of triethylene glycol bis-tosylate[59] (34.9 g, 0.076 mol) in dry tetrahydrofuran (250 ml) was added dropwise over 6 h, before refluxing for 4 days under an atmosphere of N_2. Upon cooling to room temperature hydrochloric acid (10 M, 15 ml) was added, the precipitate filtered, the solid washed well with ethyl acetate (EtOAc) and the combined solvents were removed by rotary evaporation. The residue was dissolved in EtOAc and washed (H_2O); the aqueous layer was extracted with $CHCl_3$, and the combined organic layers dried (Na_2SO_4). Purification was carried out on a silica column using CH_2Cl_2–Et_2O (4:1) + 2% EtOH as eluent to yield the desired product as a pale yellow solid which was recrystallised to yield a white solid (1.10 g, 5%), mp 125 °C (lit.,[23] 125 °C) (from ethyl acetate).

1,4,7,10,17,20,23,26-Octaoxa[10.10]-13,29-bis(hydroxymethyl)-metacyclophane 8(i)

Cyclophane **7(i)** (1.35 g, 2.39 mmol) and $LiAlH_4$ (0.54 g, 14.2 mmol) were mixed in dry tetrahydrofuran (100 ml) and stirred under N_2 at room temperature for 1.5 h. Ethyl acetate (20 ml) was then added to destroy any unreacted $LiAlH_4$, and the solvent removed by rotary evaporation. The residue was then partitioned between H_2SO_4 (20%, 100 ml) and $CHCl_3$ (100 ml). The aqueous layer was extracted with $CHCl_3$ (70 ml), and the combined organic layers washed (H_2O) and dried (Na_2SO_4). The product was recrystallised to yield a white solid (0.99 g, 81%), mp 112–113 °C (from ethanol) (Found: C, 61.29; H, 7.32. $C_{26}H_{36}O_{10}$ requires C, 61.40; H, 7.14%); δ_H(300 MHz; $CDCl_3$) 6.48 (4H, d, *J* 2, ArH), 6.35 (2H, t, *J* 2, ArH), 4.55 (4H, s, CH_2), 4.06–4.03 (8H, m, OCH_2), 3.84–3.81 (8H, m, OCH_2), 3.72 (8H, s, OCH_2) and 1.72 (2H, br s, OH).

1,4,7,10,17,20,23,26-Octaoxa[10.10]-13,29-bis(chloromethyl)-metacyclophane 9(i)

Crown ether **8(i)** (1.02 g, 2.01 mmol) and dry pyridine (18 drops) were dissolved in dry benzene (60 ml) with warming and stirring. Then thionyl chloride (0.8 ml) was added dropwise over 5 min *via* a syringe, and the resulting solution was refluxed for 55 min. The reaction mixture was poured into H_2O and the organic layer washed (H_2O), dried (Na_2SO_4) and the solvent removed by rotary evaporation. The residue was recrystallised to yield a creamy white solid (1.06 g, 97%), mp 110–112 °C (from ethanol); δ_H(300 MHz; $CDCl_3$) 6.52 (4H, d, *J* 2, ArH), 6.42 (2H, t, *J* 2, ArH), 4.46 (4H, s, CH_2), 4.07–4.04 (8H, m, OCH_2), 3.84–3.81 (8H, m, OCH_2), 3.71 (8H, s, OCH_2).

1,4,7,10,17,20,23,26-Octaoxa[10.10]-13,29-bis(2-formylphenoxymethyl)metacyclophane 10(i)

Salicylaldehyde (537 mg, 4.40 mmol) in dry degassed acetonitrile (50 ml) together with K_2CO_3 (914 mg, 6.61 mmol) was then heated at 60 °C under N_2 for 40 min before **9(i)** (1.09 g, 2.00 mmol) in dry acetonitrile (30 ml) was added and the solution was refluxed under N_2 for 6.5 h. Upon cooling the solvent was removed by rotary evaporation, the residue partitioned between H_2O and $CHCl_3$, the organic layer separated, washed (H_2O) and dried (Na_2SO_4). After removing the solvent, the solid residue was washed well with diethyl ether until no salicylaldehyde was detected by TLC. Recrystallisation yielded a white solid (1.39 g, 97%), mp 153–155 °C (from ethanol) (Found: C, 66.56; H, 6.09. $C_{40}H_{44}O_{12}$ requires C, 67.02; H, 6.19%); δ_H(300 MHz; $CDCl_3$) 10.54 (2H, s, CHO), 7.83 (2H, dd, *J* 6, 2, ArH), 7.48 (2H, dt, *J* 6, 2, ArH), 7.04–6.95 (4H, s, ArH), 6.56 (4H, d, *J* 2, ArH), 6.43 (2H, t, *J* 2, ArH), 5.06 (4H, s, CH_2), 4.08–4.04 (8H, m, α-OCH_2), 3.84–3.81 (8H, m, β-OCH_2), 3.71 (8H, s, γ-OCH_2).

Crowned porphyrin H_2STCR(3)P 4(i)a

Crown ether **10(i)** (477 mg, 0.666 mmol) and 3,3′-diethyl-4,4′-dimethyl-2,2′-dipyrrylmethane **11**[45,60] (314 mg, 1.36 mmol) were dissolved with stirring in dry acetonitrile (70 ml). The solution was then bubbled with N_2 for 30 min before adding trichloroacetic acid (100 mg) in dry tetrahydrofuran (10 ml). The reaction mixture was stirred for an additional 48 h (RT, N_2, dark), before adding *o*-chloranil (900 mg, 3.66 mmol) in dry tetrahydrofuran (15 ml) and stirring was continued overnight. The solvent was removed by rotary evaporation, and the residue partitioned between H_2O and CH_2Cl_2. The organic layer was separated, washed (sat. aq. Na_2CO_3) and dried (Na_2SO_4). Purification was carried out on an alumina column by eluting with CH_2Cl_2, followed by ethyl acetate (5%)–CH_2Cl_2 to remove impurities, followed by ethyl acetate–CH_2Cl_2 (1:9) to obtain the desired porphyrin **4(i)a** (381 mg, 50%), mp 305–307 °C (from CH_2Cl_2–MeOH); *m/z* (EMS) $(M + H)^+$, 1135.6025 (calc. 1135.5800); $(M + 2H)^{2+}$, 568.2878 (calc. 568.2939); λ_{max}(acetone)/nm 406, 504, 536, 574 and 628; δ_H(300 MHz; CD_3COCD_3) 10.22 (2H, s, H-1), 7.91 (2H, dt, *J* 7, 2, H-13), 7.90 (2H, dd, *J* 7, 2, H-11), 7.62 (2H, d, *J* 8, H-14), 7.50 (2H, dt, *J* 7, 1, H-12), 5.55 (4H + 2H, s, H-18, -22, -20), 4.97 (4H, s, H-16), 4.14–3.98 (8H, m, H-4, -4′), 2.94 (8H, s, H-25), 2.79–2.77 (8H, m, H-23), 2.70–2.68 (8H, m, H-24), 2.66 (12H, s, H-7), 1.79 (12H, t, *J* 8, H-5) and −2.43 (2H, br s, pyrrole NH); δ_C($CDCl_3$) 158.85, 158.52, 145.24, 144.11, 140.65, 137.70, 135.40, 134.54, 131.97, 130.20, 121.42, 113.87, 112.94, 105.94, 101.50, 95.91, 70.92, 70.26, 68.47, 66.29, 19.92, 17.72 and 13.77.

Zinc crowned porphyrin ZnSTCR(3)P 4(i)b

Zinc was inserted into the macrobicyclic crown porphyrin **4(i)a** using the standard procedure [$Zn(OAc)_2$/CH_2Cl_2/MeOH][61] to give **4(i)b**, which was recrystallised from CH_2Cl_2–MeOH, mp 295–296 °C (Found: C, 68.71; H, 6.15; N, 4.27. $C_{70}H_{76}N_4O_{10}Zn\cdot H_2O$ requires C, 69.09; H, 6.46; N, 4.61%); λ_{max}/nm (ε M^{-1} cm^{-1}, $CHCl_3$) 416 (3.69×10^5), 506 (3.16×10^3), 542 (1.86×10^4), 578 (8.48×10^3); δ_H(300 MHz; $CDCl_3$) 10.03 (2H, s, H-1), 7.97 (2H, dd, *J* 6, 2, ArH), 7.81 (2H, t, *J* 7, ArH), 7.46–7.42 (4H, m, ArH), 5.15 (4H, d, *J* 2, H-18, -22), 5.09 (2H, t, *J* 2, H-20), 4.81 (4H, s, H-16), 4.04–3.91 (8H, m, H-4), 2.56 (8H + 12H, s, OCH_2 + H-7), 2.47 (8H, s, OCH_2), 2.39–2.36 (8H, m, OCH_2), 1.74 (12H, t, *J* 7, H-5), 1.50 (2H, s, H_2O).

Dimethyl 1,4,7,10,13,20,23,26,29,32-decaoxa[13.13]metacyclophane-16,35-dicarboxylate 7(ii)

Methyl 3,5-dihydroxybenzoate (12.4 g, 0.074 mol) and NaH (7.1 g, 0.296 mol) were mixed in dry tetrahydrofuran (300 ml) and the solution was thoroughly degassed with N_2. The solution was then heated with stirring for 30 min under N_2, before adding tetraethylene glycol bis-tosylate[59,62] (37.2 g, 0.074 mol) in dry tetrahydrofuran (300 ml) dropwise over 5 h, then refluxing for 7 days under an atmosphere of N_2. Upon cooling to room temperature the solvent was removed by rotary evaporation and the residue was partitioned between a mixture of EtOAc, $CHCl_3$ and HCl (10 M), and filtered. The organic layer was separated and washed (H_2O); the aqueous layer was extracted with $CHCl_3$, and the combined organic layers dried (Na_2SO_4). Purification was carried out on a silica column by eluting with CH_2Cl_2, followed by diethyl ether (5%)–CH_2Cl_2 to remove the bulk of the impurities followed by diethyl ether (20%)–CH_2Cl_2 to obtain the desired product as a yellow oil. Recrystallisation yielded a white solid (1.58 g, 7%), mp 107–108 °C (lit.,[23] 106 °C) (from ethyl acetate).

1,4,7,10,13,20,23,26,29,32-Decaoxa[13.13]-16,35-bis(hydroxymethyl)metacyclophane 8(ii)

Crown ester **7(ii)** (0.97 g, 1.49 mmol) and $LiAlH_4$ (0.29 g, 7.64 mmol) were mixed in dry tetrahydrofuran (80 ml) and stirred under N_2 at room temperature for 1.5 h. The solvent was then removed by rotary evaporation and the residue partitioned between HCl (2 M) and $CHCl_3$, and the organic phase separated. The aqueous layer was extracted with $CHCl_3$, and the combined organic layers washed (H_2O) and dried (Na_2SO_4). The product was recrystallised to yield a white solid (0.74 g, 83%), mp 77–78 °C (from ethyl acetate) (Found: C, 58.72; H, 7.94. $C_{30}H_{44}O_{12}\cdot H_2O$ requires C, 58.62; H, 7.54%); δ_H(300 MHz; $CDCl_3$) 6.49 (4H, d, *J* 2, ArH), 6.34 (2H, t, *J* 2, ArH), 4.55 (4H, d, *J* 5, CH_2), 4.04–4.01 (8H, m, OCH_2), 3.83–3.80 (8H, m, OCH_2), 3.72–3.66 (16H, m, OCH_2), 1.98 (2H, t, *J* 5, OH), 1.56 (2H, s, H_2O).

1,4,7,10,13,20,23,26,29,32-Decaoxa[13.13]-16,35-bis(chloromethyl)metacyclophane 9(ii)

Alcohol **8(ii)** (0.55 g, 0.92 mol) and dry pyridine (9 drops) were dissolved in dry benzene (30 ml) with heating and stirring and thionyl chloride (0.4 ml) was added dropwise over 1 min *via* a syringe before refluxing for 1 h. Upon cooling to room temperature, the reaction mixture was poured into H_2O and the organic layer washed (2 M aq. HCl), then dried (Na_2SO_4) and the solvent removed by rotary evaporation. The residue was recrystallised to yield a beige solid (0.42 g, 72%), mp 95–96 °C (from ethyl acetate) (Found: C, 56.57; H, 6.52. $C_{30}H_{42}Cl_2O_{10}$ requires C, 56.87; H, 6.68%); δ_H(300 MHz; $CDCl_3$) 6.51 (4H, d, *J* 2, ArH), 6.40 (2H, t, *J* 2, ArH), 4.45 (4H, s, CH_2), 4.06–4.03 (8H, m, OCH_2), 3.83–3.80 (8H, m, OCH_2), 3.71–3.66 (16H, m, OCH_2).

1,4,7,10,13,20,23,26,29,32-Decaoxa[13.13]-16,35-bis(2-formylphenoxymethyl)metacyclophane 10(ii)

A solution of salicylaldehyde (0.33 g, 2.74 mmol) in dry acetonitrile (40 ml) along with K_2CO_3 (0.86 g, 6.24 mmol) was degassed with N_2 and heated for 30 min under N_2 before **9(ii)** (0.79 g, 1.25 mmol) in dry acetonitrile (60 ml) was added all at once. The solution was degassed again, and the reaction mixture refluxed under N_2 overnight (13 h). Upon cooling, the solvent was removed by rotary evaporation, the residue partitioned between H_2O and $CHCl_3$, the organic layer separated, washed (2 M aq. NaOH) and dried (Na_2SO_4). The residue was recrystallised to yield a pale brown solid (0.78 g, 78%), mp 107 °C (from ethyl acetate) (Found: C, 64.12; H, 6.60. $C_{44}H_{52}O_{14}\cdot H_2O$ requires C, 64.22; H, 6.61%); δ_H(300 MHz; $CDCl_3$) 10.54 (2H, s, CHO), 7.83 (2H, d, *J* 8, ArH), 7.48 (2H, d, *J* 8, ArH), 7.01 (2H, t, *J* 7, ArH), 6.96 (2H, d, *J* 8, ArH), 6.55 (4H, s, ArH), 6.42 (2H, s, ArH), 4.04–4.03 (8H, m, OCH_2), 3.84–3.82 (8H, m, OCH_2), 3.69–3.68 (16H, m, OCH_2).

Crowned porphyrin H_2STCR(4)P 4(ii)a

Bis-aldehyde **10(ii)** (0.48 g, 0.60 mmol) and 3,3′-diethyl-4,4′-dimethyl-2,2′-dipyrrylmethane[45,60] (0.27 g, 1.19 mmol) were dissolved with stirring in dry acetonitrile (60 ml). The solution was then bubbled with N_2 for 40 min before adding trichloroacetic acid (~200 mg). The reaction mixture was then stirred for an additional 48 h (RT, N_2, dark), before adding *o*-chloranil (0.44 g, 1.79 mmol) in dry tetrahydrofuran (15 ml) and stirring was continued overnight. The solvent was removed by rotary evaporation, and the residue partitioned between $CHCl_3$ and sat. aq. $NaHCO_3$; the organic layer was separated, washed (sat. aq. Na_2CO_3) and dried (Na_2SO_4). An initial purification was carried out on a chromatotron by eluting with CH_2Cl_2, followed by MeOH (1%)–CH_2Cl_2 then MeOH (2%)–CH_2Cl_2. A final purification was carried out on preparative TLC plates with MeOH (2%)–CH_2Cl_2 as the eluent to obtain the desired porphyrin. The product was recrystallised to obtain a purple–red solid (0.129 g, 18%), mp 184–186 °C (from CH_2Cl_2–MeOH) (Found: C, 72.19; H, 7.06; N, 4.32. $C_{74}H_{86}O_{12}N_4$ requires C, 72.64; H, 7.08; N, 4.58%); *m/z* (EMS) $(M + H)^+$ 1223.6498 (calc. 1223.6325); $(M + 2H)^{2+}$, 612.3211 (calc. 612.3201); λ_{max}(acetone)/nm 407, 504, 538, 574, 628; δ_H(300 MHz; CD_3COCD_3) 10.25 (2H, s, H-1), 7.91 (2H, t, *J* 8, H-13), 7.89 (2H, d, *J* 7, H-11), 7.60 (2H, d, *J* 8, H-14), 7.49 (2H, t, *J* 7, H-12), 5.55 (2H, t, *J* 2, H-20), 5.34 (4H, d, *J* 2, H-18, -22), 5.07 (4H, s, H-16), 4.05 (8H, q, *J* 8, H-4), 2.85–2.82 (8H, m, H-26), 2.64 (12H, s, H-7), 2.54–2.51 (8H, m, H-25), 2.19–2.17 (8H, m, H-23), 1.93–1.90 (8H, m, H-24), 1.79 (12H, t, *J* 8, H-5), −2.32 (2H, s, pyrrole NH); δ_C($CDCl_3$) 158.72, 158.55, 145.23, 144.38, 140.74, 138.15, 135.58, 134.20, 131.92, 130.32, 121.44, 114.04, 112.65, 104.30, 101.24, 96.02, 70.24, 70.05, 69.89, 67.76, 65.37, 19.98, 17.68, 13.76.

Zinc crowned porphyrin ZnSTCR(4)P 4(ii)b

Zinc was inserted into the macrobicyclic crowned porphyrin **4(ii)a** using standard procedures [$Zn(OAc)_2$/CH_2Cl_2/MeOH][61] to give **4(ii)b** which was recrystallised from CH_2Cl_2–MeOH, mp 216–217 °C; λ_{max}/nm 414, 506, 542, 578; δ_H(300 MHz; CD_3COCD_3) 10.17 (2H, s, H-1), 7.88–7.83 (4H, m, H-11 + H-13), 7.53 (2H, d, *J* 8, H-14), 7.44 (2H, t, *J* 7, H-12), 5.74 (2H, t, *J* 2, H-20), 5.68 (4H, d, *J* 2, H-18, -22), 4.96 (4H, s, H-16), 4.10 (4H, q, *J* 8, H-4), 3.99 (4H, q, *J* 8, H-4′), 3.13–3.10 (8H, m, H-23), 2.61–2.58 (8H, m, H-24), 2.58 (12H, s, H-7), 1.82 (12H, t, *J* 8, H-5), 1.52 (8H, s, H-25), 1.22 (8H, s, H-26).

1,8-Bis[4-(hydroxymethyl)phenoxy]-3,6-dioxaoctane 12

4-Hydroxybenzyl alcohol (7.05 g, 0.057 mol) and anhydrous K_2CO_3 (23.5 g, 0.17 mol) were dissolved in dry MeCN (190 ml) and the solution was degassed with N_2. The solution was then heated with stirring for 30 min under N_2, before adding triethylene glycol bis-tosylate[62] **2a** (13.0 g, 0.028 mol) in dry MeCN (100 ml) all at once, and then refluxing under N_2 for 60 h. Upon cooling to room temperature the solvent was removed by rotary evaporation and the residue partitioned between CH_2Cl_2 and H_2O, the organic layer separated, washed (H_2O), dried (Na_2SO_4), and the solvent removed by rotary evaporation. The solid obtained was then purified by recrystallisation to yield a creamy white solid (7.03 g, 68%), mp 94–98 °C (from $CHCl_3$–Et_2O) (Found: C, 66.02; H, 6.97. $C_{20}H_{26}O_6$ requires C, 66.28; H, 7.23%); δ_H(300 MHz; $CDCl_3$) 7.21 (4H, d, *J* 9, ArH), 6.86 (4H, dd, *J* 9, 2, ArH), 4.55 (4H, s, CH_2), 4.09 (4H, t, *J* 5, OCH_2), 3.83 (4H, t, *J* 5, OCH_2), 3.72 (4H, s, OCH_2), 2.08 (2H, br s, OH).

1,8-Bis[4-(chloromethyl)phenoxy]-3,6-dioxaoctane 13

Alcohol **12** (3.08 g, 8.50 mmol) and dry pyridine (1.48 g, 18.7 mmol) were heated with stirring at reflux in dry benzene (50 ml), before adding thionyl chloride (2.55 g, 21.4 mmol) dropwise over 4 min, then refluxing for an additional 2 h. Upon cooling to room temperature, the reaction mixture was poured into H_2O and the aqueous layer extracted with ethyl acetate. The combined organic layers were then washed (H_2O), dried (Na_2SO_4) and the solvent evaporated to yield a yellow oil which solidified upon standing (3.18 g, 94%), mp 68–71 °C and which was used without further purification; δ_H(300 MHz; $CDCl_3$) 7.28 (4H, dd, *J* 9, 2, ArH), 6.87 (4H, dd, *J* 9, 2, ArH), 4.55 (4H, s, CH_2), 4.11 (4H, t, *J* 5, OCH_2), 3.85 (4H, t, *J* 5, OCH_2), 3.74 (4H, s, OCH_2).

1,8-Bis{4-[(2-formyl)phenoxymethyl]phenoxy}-3,6-dioxaoctane 14

Salicylaldehyde (1.71 g, 14.0 mmol) and K_2CO_3 (4.40 g, 31.8 mmol) were dissolved in dry acetonitrile (50 ml) and the solution degassed with N_2. The solution was then heated for 30 min under N_2 before **13** (2.54 g, 6.36 mmol) in dry acetonitrile (90 ml) was added all at once, the solution was degassed again, and the reaction mixture refluxed under N_2 overnight. Upon cooling, the solvent was removed by rotary evaporation, the residue partitioned between CH_2Cl_2 and H_2O, the organic layer separ-

ated, washed (2 M aq. NaOH) and dried (Na_2SO_4). The solvent was evaporated to yield a yellow oil (3.36 g, 93%) (Found: C, 71.30; H, 6.35. $C_{34}H_{34}O_8$ requires C, 71.56; H, 6.01%); δ_H(300 MHz; $CDCl_3$) 10.50 (2H, s, CHO), 7.83 (2H, dd, *J* 8, 2, ArH), 7.51 (2H, dt, *J* 8, 2, ArH), 7.32 (4H, d, *J* 9, ArH), 7.04 (2H, d, *J* 9, ArH), 7.02 (2H, t, *J* 9, ArH), 6.93 (4H, d, *J* 9, ArH), 5.09 (4H, s, CH_2), 4.13 (4H, t, *J* 5, OCH_2), 3.86 (4H, t, *J* 5, OCH_2), 3.75 (4H, s, OCH_2).

Strapped porphyrin H_2ST(3)P 6a

A solution of aldehyde **14** (430 mg, 0.75 mmol) and 3,3′-diethyl-4,4′-dimethyl-2,2′-dipyrrylmethane[45,60] (347 mg, 1.51 mmol) in dry acetonitrile (75 ml) was then bubbled with N_2 for 10 min before adding catalytic amounts of trichloroacetic acid in dry THF (25 ml) and bubbling N_2 for a further 3 min. The reaction mixture was then stirred for an additional 48 h (RT, N_2, dark), before adding *o*-chloranil (927 mg, 3.77 mmol) in dry tetrahydrofuran (30 ml) and stirring was continued overnight. The solvent was removed by rotary evaporation, and the residue partitioned between CH_2Cl_2 and aq. $NaHCO_3$, filtered, the organic layer separated, washed (sat. aq. Na_2CO_3) and dried (Na_2SO_4). Purification was carried out on an alumina column by eluting with CH_2Cl_2, followed by EtOAc (2%)–CH_2Cl_2 to obtain the desired porphyrin. The product was recrystallised to obtain a purple–red solid (153 mg, 21%), mp 268–270 °C (from CH_2Cl_2–MeOH) (Found: C, 76.31; H, 7.16; N, 5.36. $C_{64}H_{68}N_4O_6{\cdot}H_2O$ requires C, 76.31; H, 7.01; N, 5.56%); *m*/*z* (EMS) $(M + H)^+$, 989.5168 (calc. 989.522 07); $(M + 2H)^{2+}$, 495.2599 (calc. 495.264 95); λ_{max}(acetone)/nm 406, 504, 536, 574, 628; δ_H(300 MHz; $CDCl_3$) 10.16 (2H, s, H-1), 7.79 (2H, dt, *J* 7, 2, H-13), 7.59 (2H, dd, *J* 7, 2, H-11), 7.46 (2H, d, *J* 8, H-14), 7.32 (2H, t, *J* 7, H-12), 6.50 (4H, d, *J* 9, H-18, -22), 6.08 (4H, d, *J* 9, H-19, -21), 5.15 (4H, s, CH_2), 4.00 (8H, q, *J* 7, H-4), 3.55–3.52 (4H, m, H-23), 3.43–3.40 (4H, m, H-24), 3.32 (4H, s, H-25), 2.58 (12H, s, H-7), 1.76 (12H, t, *J* 7, H-5), 1.52 (2H, s, H_2O), −2.35 (2H, br s, pyrrole NH); δ_C($CDCl_3$) 158.51, 157.56, 145.34, 144.18, 140.79, 135.39, 135.00, 131.73, 130.03, 128.78, 127.69, 121.08, 113.96, 113.80, 111.87, 96.01, 70.49, 69.93, 69.14, 67.06, 19.92, 17.68, 13.63.

Strapped porphyrin ZnST(3)P 6b

Zinc was inserted into the macrocyclic strapped porphyrin **6a** using the standard procedure [$Zn(OAc)_2$/CH_2Cl_2/MeOH][61] to give **6b** which was recrystallised from CH_2Cl_2–MeOH, mp >350 °C; λ_{max}/nm (ε M^{-1} cm^{-1}) [DMSO (1%)–MeCN] 416 (3.75×10^5), 506 (2.39×10^3), 544 (1.66×10^4), 582 (4.49×10^3); δ_H[300 MHz; CD_3SOCD_3 (20%)–CD_3COCD_3] 10.07 (2H, s, H-1), 7.86 (2H, dt, *J* 7, 2, H-13), 7.67 (2H, d, *J* 8, H-14), 7.52 (2H, d, *J* 7, H-11), 7.36 (2H, t, *J* 7, H-12), 6.63 (4H, d, *J* 9, H-18, -22), 6.12 (4H, d, *J* 9, H-19, -21), 5.23 (4H, s, CH_2), 4.00 (8H, q, *J* 7, H-4), 3.57–3.54 (4H, m, H-23), 3.39–3.36 (4H, m, H-24), 3.26 (4H, s, H-25), 2.57 (12H, s, H-7), 1.74 (12H, t, *J* 7, H-5).

Determination of association constants

Association constants were determined by NMR titrations as the data fitted in a non-linear least-squares procedure as previously described.[23] Although errors for individual association constants are not quoted, the values should be viewed as containing at least a 10% uncertainty.[63,64]

Structure determinations

Crystals of complex **4(i)b·PQ^{2+}** decomposed rapidly upon removal from the mother liquor, and the data collection was accordingly undertaken at a temperature of −115 °C. A purple tabular crystal having approximate dimensions of 0.47 × 0.40 × 0.10 mm was attached to a glass fibre with Paratone[65] and quenched in a nitrogen gas cold stream on mounting on a Rigaku AFC7R diffractometer equipped with a Molecular Structure Corporation low temperature system. Graphite monochromated Cu-Kα radiation was used for the diffraction data collection, and the radiation was generated with a rotating anode. Primitive monoclinic cell constants were obtained from a least-squares refinement using the setting angles of 25 reflections in the range $18.67 < 2\theta < 23.30°$. Omega scans of several intense reflections made prior to data collection, had an average width at half-height of 0.13°. Profile data were collected to 100° 2θ, with backgrounds obtained with a Learman–Larsen routine,[66] and data beyond 100° 2θ to 130.2° 2θ were collected conventionally with $\omega - 2\theta$ scans of $(1.50 + 0.35)\tan(\theta)°$ width and a speed of 32.0° min^{-1} (in omega). Obvious signs of an imminent blockage to the cold stream resulted in two interruptions to the data collection, with the crystal being quickly transferred to a dry ice box while the blockages were cleared. The three overlapping data sets were merged, with first data set comprising 9416 reflections of which 8896 were independent (R_{merge} = 8%), the second set contained 919 reflections with 896 being independent (R_{merge} = 4.7%) and the third set had 2768 with 2741 independent reflections (R_{merge} = 18.4%). The final number of independent reflections obtained from the 13 103 collected reflections was 12 091. An analytical absorption correction was applied and the data were also corrected for Lorentz and polarisation effects.

In general, data processing and calculations were undertaken with the TEXSAN[67] crystallographic software package, however least-squares planes and lines were calculated with the XTAL[68] crystallographic program suite. Neutral atom scattering factors were taken from Cromer and Waber.[69] Anomalous dispersion effects were included in F_{calc}[70] and the values for Δf′ and Δf″ were those of Creagh and McAuley.[71] The values for the mass attenuation coefficients were those of Creagh and Hubbell.[72] The structure was solved in the space group $P2_1/n$ (#14) by direct methods[73] and expanded using Fourier techniques.[74] In general the non-hydrogen atoms were modelled anisotropically, and hydrogen atoms were included in the model at calculated positions with group thermal parameters. There was orientational disorder in one of the straps, with two sites being modelled for O(8), C(67) and C(68) with complementary populations of 0.6 and 0.4 (the populations were refined and then fixed at the first decimal place). In addition to a coordinated acetonitrile molecule, the refined model included a fully occupied acetonitrile solvate site and a 0.4 occupancy acetonitrile solvate site. Three residual peaks in the difference map were attributed to oxygen atoms of partially occupied water sites. No hydrogens were included in the model for the partially occupied solvate and water sites.

Crystal data for complex 4(i)b·PQ^{2+}

Single crystals suitable for X-ray analysis were obtained by slow diffusion of diisopropyl ether into a solution of **4(i)b** and **PQ^{2+}(PF_6)$_2$** in chloroform and acetonitrile. Refined model formula $C_{86.8}H_{94.4}F_{12}N_{8.4}O_{10.9}P_2Zn$, purple blade 0.475 × 0.4 × 0.10 mm, monoclinic, space group $P2_1/n$ (#14) a = 15.047(3), b = 24.288(3), c = 23.567(4) Å, β = 103.66(1)°, V = 8369(2) Å^3, D_c(Z = 4) = 1.410 g cm^{-3}, λ(Cu-Kα) = 1.5406 Å, μ(Cu-Kα) = 15.62 cm^{-1}, analytical absorption min., max. = 0.61, 0.86, F(000) = 3716.80 electrons. Ranges of *hkl* 0–17, 0–26, −26 to 26; 4 to 130° 2θ, N = 13 103, N(unique) = 12 091, R_{merge} = 0.083, N_o = 9600 [$I > 3.0\sigma(I)$], N_{var} = 1093, R = 0.062, R_w = 0.059, residual extrema −0.72 to 0.64.

Single crystals of **5b·PQ^{2+}** were grown by slow diffusion at 0 °C of diisopropyl ether into a solution of **5b** and **PQ^{2+}(PF_6)$_2$** in acetone. A small purple blade like crystal of complex **5b·PQ^{2+}**, having approximate dimensions of 0.09 × 0.09 × 0.01 mm, was attached to a thin glass fibre, and mounted on the diffractometer mentioned above. Primitive monoclinic cell constants were obtained from a least-squares refinement using the setting angles of 25 reflections in the range $18.59 < 2\theta < 27.21°$. Diffraction data were collected at a temperature of 21 ± 1 °C using ω−2θ scans to a maximum 2θ value of 110.2°. Omega scans of several intense reflections made prior to data

collection, had an average width at half-height of 0.19°, and scans of (1.63 + 0.35 tan θ)° were made at a speed of 32.0° min^{-1} (in omega). The weak reflections [$I < 15.0\,\sigma(I)$] were rescanned up to 10 times. Stationary background counts were recorded on each side of the reflection, with a 2:1 ratio of peak to background counting time. The intensities of three representative reflections measured every 150 reflections, did not change significantly during the data collection. An empirical absorption correction based on azimuthal scans of three reflections was applied and the data were also corrected for Lorentz and polarisation effects.

The structure was solved by heavy-atom Patterson methods[75] and expanded using Fourier techniques.[74] The data obtained from the crystal was of comparatively poor quality and only 17.4% of the unique data was classified as observed. Consequently only the zinc and phosphorus atoms were modelled with anisotropic thermal parameters. Hydrogen atoms were included in the model at calculated positions with group thermal parameters. The refinement model included seven partially occupied oxygen sites, with a total occupancy of 2.5, attributed to water molecules. No water hydrogen atoms were included in the model. One of the PF_6^- ions were disordered and was modelled with seven fluorine sites. Large thermal parameters for the C(36)–C(37) ethyl residue suggest that this group suffers high thermal motion or may be disordered above and below the porphyrin plane. Restraints were applied to the C(7)–C(36), C(13)–C(40), C(17)–C(42) and C(27)–C(28) bond lengths.

Crystal data for complex 5b·PQ^{2+}

Refined model formula $C_{78}H_{86}F_{12}N_6O_{10.5}P_2Zn$, purple blade 0.087 × 0.087 × 0.013 mm, monoclinic, space group $P2_1/c$ (#14), $a = 17.869(8)$, $b = 18.024(6)$, $c = 26.692(9)$ Å, $\beta = 102.15(4)°$, $V = 8404(5)$ Å^3, $D_c(Z = 4) = 1.289$ g cm^{-3}, λ(Cu-Kα) = 1.5406 Å, μ(Cu-Kα) = 14.92 cm^{-1}, psi scan absorption min., max. = 0.73–0.99, $F(000) = 3392.00$ electrons. Ranges of *hkl* 0–17, 0–19, −28 to 27; 4 to 111° 2θ, $N = 10\,146$, N(unique) = 9701, $R_{merge} = 0.169$, $N_o = 1692$ [$I > 2.0\sigma(I)$], $N_{var} = 476$, $R = 0.121$, $R_w = 0.127$, residual extrema −0.42 to 0.59.

Atomic coordinates, thermal parameters and geometrical details for both crystal structures have been deposited at the Cambridge Crystallographic Data Centre (CCDC). For details of the deposition scheme, see 'Instructions for Authors', *J. Chem. Soc., Perkin Trans. 1*, available *via* the RSC Web page (http://www.rsc.org/authors). Any request to the CCDC for this material should quote the full literature citation and the reference number 207/216.

Acknowledgements

Support by the Australian Research Council for part of this work is acknowledged, as is David Tucker for assistance with NMR measurements. We thank Trevor W. Hambley for support for the crystallographic structure determinations.

References

1 V. Balzani and F. Scandola, in *Supramolecular Photochemistry*, Ellis Horwood, Chichester, 1991.
2 V. Balzani, *Tetrahedron*, 1992, **48** (Tetrahedron Report No. 326), 10 443.
3 V. Balzani and F. Scandola, in *Comprehensive Supramolecular Chemistry*, ed. D. N. Reinhoudt, Pergamon, Oxford, England, 1996, vol. 10, pp. 687–746.
4 J.-M. Lehn, in *Supramolecular Chemistry*: *Concepts and Perspectives*, VCH, Weinheim, 1995.
5 L. Fabbrizzi and A. Poggi, *Chem. Soc. Rev.*, 1995, 197.
6 M. R. Wasielewski, *Chem. Rev.*, 1992, **92**, 435.
7 I. Willner and B. Willner, *Top. Curr. Chem.*, 1991, **159**, 157.
8 D. Gust and T. A. Moore, *Top. Curr. Chem.*, 1991, **159**, 103.
9 I. Willner and B. Willner, in *Advances in Photochemistry*, ed. D. C. Neckers, D. H. Volman and G. v. Brünau, 1995, vol. 20, p. 217.
10 T. A. Moore, D. Gust, A. L. Moore, R. V. Benasson, P. Seta and E. Bienvenue, in *Supramolecular Photochemistry*, ed. V. Balzani and D. Reidel, Boston, 1987, p. 283.
11 J. S. Connolly and J. R. Bolton, in *Photoinduced Electron Transfer*, *Part D*, ed. M. A. Fox and M. Chanon, Elsevier, Amsterdam, 1988, p. 303.
12 J. L. Sessler, B. Wang, S. L. Springs and C. T. Brown, in *Comprehensive Supramolecular Chemistry*, ed. Y. Murakami, Pergamon, Oxford, England, 1996, vol. 4, p. 311.
13 A. C. Benniston and A. Harriman, *J. Am. Chem. Soc.*, 1994, **116**, 11 531.
14 A. C. Benniston, A. Harriman, D. Philp and J. F. Stoddart, *J. Am. Chem. Soc.*, 1993, **115**, 5298.
15 C. Turró, C. K. Chang, G. E. Leroi, R. I. Cukier and D. G. Nocera, *J. Am. Chem. Soc.*, 1992, **114**, 4013.
16 T. Hayashi, T. Miyahara, N. Hashizume and H. Ogoshi, *J. Am. Chem. Soc.*, 1993, **115**, 2049.
17 Y. Kuroda, M. Ito, T. Sera and H. Ogoshi, *J. Am. Chem. Soc.*, 1993, **115**, 7003.
18 J.-P. Collin, A. Harriman, V. Heitz, F. Odobel and J.-P. Sauvage, *J. Am. Chem. Soc.*, 1994, **116**, 5679.
19 M. Kropf, E. Joselevich, H. Dürr and I. Willner, *J. Am. Chem. Soc.*, 1996, **118**, 655.
20 M. J. Gunter and M. R. Johnston, *Tetrahedron Lett.*, 1990, **31**, 4801.
21 M. J. Gunter and M. R. Johnston, *Tetrahedron Lett.*, 1992, **33**, 1771.
22 M. J. Gunter, M. R. Johnston, B. W. Skelton and A. H. White, *J. Chem. Soc., Perkin Trans. 1*, 1994, 1009.
23 M. J. Gunter and M. R. Johnston, *J. Chem. Soc., Perkin Trans. 1*, 1994, 995.
24 E. Zahavy, M. Seiler, S. Marx-Tibbon, E. Joselevich, I. Willner, H. Dürr, D. O'Connor and A. Harriman, *Angew. Chem., Int. Ed. Engl.*, 1995, **34**, 1005.
25 I. Willner, E. Kaganer, E. Joselevich, H. Dürr, D. David, M. J. Gunter and M. R. Johnston, *Coord. Chem. Rev.*, 1998, in the press.
26 J. L. Sessler, B. Wang and A. Harriman, *J. Am. Chem. Soc.*, 1995, **117**, 704.
27 A. Harriman, Y. Kubo and J. L. Sessler, *J. Am. Chem. Soc.*, 1992, **114**, 388.
28 J.-C. Chambron, A. Harriman, V. Heitz and J.-P. Sauvage, *J. Am. Chem. Soc.*, 1993, **115**, 6109.
29 A. Berman, E. S. Izraeli, H. Levanon, B. Wang and J. L. Sessler, *J. Am. Chem. Soc.*, 1995, **117**, 8252.
30 C. A. Hunter and R. K. Hyde, *Angew. Chem., Int. Ed. Engl.*, 1996, **35**, 1936.
31 T. Arimura, C. T. Brown, S. L. Springs and J. L. Sessler, *Chem. Commun.*, 1996, 2293.
32 J. N. H. Reek, A. E. Rowan, R. de Gelder, P. T. Beurskens, M. J. Crossley, S. D. Feyter, F. de Schryver and R. J. M. Nolte, *Angew. Chem., Int. Ed. Engl.*, 1997, **36**, 361.
33 T. Hayashi, T. Miyahara, N. Koide, Y. Kato, H. Masuda and H. Ogoshi, *J. Am. Chem. Soc.*, 1997, **119**, 7281.
34 M. J. Gunter, D. C. R. Hockless, M. R. Johnston, B. W. Skelton and A. H. White, *J. Am. Chem. Soc.*, 1994, **116**, 4810.
35 B. L. Allwood, F. H. Kohnke, J. F. Stoddart and D. J. Williams, *Angew. Chem., Int. Ed. Engl.*, 1985, **24**, 581.
36 H. M. Colquhoun, E. P. Goodings, J. M. Maud, J. F. Stoddart, J. B. Wolstenholme and D. J. Williams, *J. Chem. Soc., Perkin Trans. 2*, 1985, 607.
37 F. H. Kohnke, J. F. Stoddart, B. L. Allwood and D. J. Williams, *Tetrahedron Lett.*, 1985, **26**, 1681.
38 B. L. Allwood, H. Shahriari-Zavareh, J. F. Stoddart and D. J. Williams, *J. Chem. Soc., Chem. Commun.*, 1987, 1058.
39 P. R. Ashton, E. J. T. Chrystal, J. P. Mathias, K. P. Parry, A. M. Z. Slawin, N. Spencer, J. F. Stoddart and D. J. Williams, *Tetrahedron Lett.*, 1987, **28**, 6367.
40 B. L. Allwood, N. Spencer, H. Shahriari-Zavareh, J. F. Stoddart and D. J. Williams, *J. Chem. Soc., Chem. Commun.*, 1987, 1061.
41 B. L. Allwood, N. Spencer, H. Shahriari-Zavareh, J. F. Stoddard and D. J. Williams, *J. Chem. Soc., Chem. Commun.*, 1987, 1064.
42 B. L. Allwood, H. M. Colquhoun, S. M. Doughty, F. H. Kohnke, A. M. Z. Slawin, J. F. Stoddart, D. J. Williams and R. Zarzycki, *J. Chem. Soc., Chem. Commun.*, 1987, 1054.
43 P. R. Ashton, A. M. Z. Slawin, N. Spencer, J. F. Stoddart and D. J. Williams, *J. Chem. Soc., Chem. Commun.*, 1987, 1066.
44 E. Kaganar, E. Joselevich, I. Willner, Z. Chen, M. J. Gunter, T. P. Jeynes and M. R. Johnston, *J. Phys. Chem. B*, 1998, **102**, 1159.
45 M. J. Gunter and L. N. Mander, *J. Org. Chem.*, 1981, **46**, 4792.
46 S. B. Ferguson, E. M. Sanford, E. M. Seward and F. Diederich, 1991, **113**, 5410.
47 D. B. Smithrud, T. B. Wyman and F. Diederich, 1991, **113**, 5420.
48 D. B. Smithrud and F. Diederich, *J. Am. Chem. Soc.*, 1990, **112**, 339.

49 ORTEP: *ORTEPII. Report ORNL-5138*, C. K. Johnson, 1976, Oak Ridge National Laboratory, Oak Ridge, Tennessee.
50 W. R. Scheidt and Y. J. Lee, *Struct. Bonding*, 1987, **64**, 1.
51 M. O. Senge, C. J. Medforth, T. P. Forsyth, D. A. Lee, M. M. Olmstead, W. Jentzen, R. K. Pandey, J. A. Shelnutt and K. M. Smith, *Inorg. Chem.*, 1997, **36**, 1149.
52 H. L. Anderson, A. Bashall, K. Henrick, M. McPartlin and J. K. M. Sanders, *Angew. Chem.*, *Int. Ed. Engl.*, 1994, **33**, 429.
53 P. Bhyrappa, V. Krishnan and M. Nethaji, *J. Chem. Soc.*, *Dalton Trans.*, 1993, 1901.
54 J. A. Castro, J. Romero, J. A. Garcia-Vazquez, A. Marcia, A. Sousa and U. Englert, *Polyhedron*, 1993, **12**, 1391.
55 I. Dance, in *The Crystal as a Supramolecular Entity*, ed. G. R. Desiraju, Wiley, Chichester, 1996, vol. 2, p. 168.
56 J. Singh and J. M. Thornton, *FEBS Lett.*, 1985, **191**, 1.
57 C. A. Hunter, *Philos. Trans. R. Soc. London*, *Ser. A*, 1993, **345**, 77.
58 C. A. Hunter and J. K. M. Sanders, *J. Am. Chem. Soc.*, 1990, **112**, 5525.
59 J. Dale and P. O. Kristiansen, *Acta Chem. Scand.*, 1972, **26**, 1471.
60 R. Young and C. K. Chang, *J. Am. Chem. Soc.*, 1985, **107**, 898.
61 K. M. Smith, *Porphyrins and Metalloporphyrins*, Elsevier, Amsterdam, 1975, ch. 5.
62 C. J. Walter and J. K. M. Sanders, *Angew. Chem.*, *Int. Ed. Engl.*, 1995, **34**, 217.
63 C. T. Seto and G. M. Whitesides, *J. Am. Chem. Soc.*, 1993, **115**, 905.
64 T. Wang, J. S. Bradshaw and R. M. Izatt, *J. Heterocycl. Chem.*, 1994, **31**, 1097.
65 H. Hope, *Acta Crystallogr.*, *Sect. B*, 1988, **44**, 22.
66 M. S. Lehmann and F. K. Larsen, *Acta Crystallogr.*, 1974, **A30**, 580.
67 TEXSAN: *Crystal Structure Analysis Package*, Molecular Structure Corporation, USA, 1985 and 1992.
68 XTAL3.4: *The XTAL 3.4 Reference Manual*, S. R. Hall, H. D. Flack and J. M. Stewart, 1992, Universities of Western Australia, Geneva and Maryland.
69 D. T. Cromer and J. T. Waber, *International Tables for X-ray Crystallography*, The Kynoch Press, Birmingham, England, Table 2.2A, 1974.
70 J. A. Ibers and W. C. Hamilton, *Acta Crystallogr.*, 1964, **17**, 781.
71 D. C. Creagh and W. J. McAuley, in *International Tables for Crystallography*, ed. A. J. C. Wilson, Kluwer Academic, Boston, 1992, vol. C, pp. 200–206, Table 4.2.6.8.
72 D. C. Creagh and J. H. Hubbell, in *International Tables for Crystallography*, ed. A. J. C. Wilson, Kluwer Academic, Boston, 1992, vol. C, pp. 200–206, Table 4.2.4.3.
73 SIR92: A. Altomare, M. Cascarano, C. Giacovazzo and A. Guagliardi, *J. Appl. Crystallogr.*, 1993, **26**, 343.
74 DIRDIF94: *The Dirdif 94 Program System – Technical Report of the Crystallography Laboratory*, P. T. Beurskens, G. Admiraal, G. Beurskens, W. P. Bosman, R. de Gelder, R. Israel and J. M. M. Smits, 1994, University of Nijmegen, The Netherlands.
75 SAPI91: Fan Hai-Fu, *Structure Analysis Programs with Intelligent Control*, Rigaku Corporation, Tokyo, Japan, 1991.

Paper 8/01302K
Received 16*th February* 1998
Accepted 16*th April* 1998